

Coupling to continuum effects in the ${}^{6,7}\text{Li} + {}^{64}\text{Zn}$ reactions at energies around the Coulomb barrier.

J. P. Fernández-García¹, M. Zadro², A. Di Pietro¹, P. Figuera¹, M. Fisichella¹, M. Lattuada^{1,4}, A. M. Moro³ and D. Torresi^{1,4}

¹INFN, Laboratori Nazionali del Sud, via S. Sofia 62, I-95123 Catania, Italy

²Ruder Bošković Institute, Bijenička cesta 54, HR-10000 Zagreb, Croatia

³Departamento de FAMN, Universidad de Sevilla, Apartado 1065, E-41080 Seville, Spain

⁴Dipartimento di Fisica e Astronomia, via S. Sofia 64, I-95123 Catania, Italy

E-mail: fernandez@lns.infn.it

Abstract.

The elastic scattering angular distributions for the weakly bound nuclei ${}^6\text{Li}$ and ${}^7\text{Li}$ on ${}^{64}\text{Zn}$ were measured in a wide angular range at energies around the Coulomb barrier. In addition, the excitation functions of quasi-elastic scattering at backward angles were measured and the corresponding barrier distributions were derived. The experimental data were analysed within the continuum-discretized-coupled-channel method. In this contribution, we will present a detailed study concerning the effects of the break-up channels in the ${}^{6,7}\text{Li} + {}^{64}\text{Zn}$ reactions.

1. Introduction

Many efforts have been concentrated on the study of nuclear collisions at energies around the Coulomb barrier induced by the halo and stable weakly bound nuclei, such as ${}^6\text{Li}$ and ${}^7\text{Li}$ (see, e.g. Ref. [1] and references therein). In fact, the coupling to the break-up channel can affect the reaction dynamics and, therefore, strong effects on elastic scattering (e.g. [2–4]) and fusion (e.g. [5, 6]) have been observed.

The barrier distribution method has been proposed as a powerful tool to study the effects of couplings to different reaction channels at near-barrier energies [7–9]. The barrier distribution of quasi-elastic scattering (D_{qel}) is defined as [10],

$$D_{qel}(E) = -\frac{d}{dE} \left[\frac{d\sigma_{qel}}{d\sigma_{Ruth}} \right], \quad (1)$$

where $d\sigma_{qel}/d\sigma_{Ruth}$ corresponds to the ratio of the quasi-elastic (QEL) scattering and the Rutherford differential cross sections at a fixed backward angle. QEL scattering is defined as the sum of elastic and inelastic scattering, and all other direct processes. In Refs. [11–14], excitation functions for QEL and/or elastic scattering at backward angles, and the corresponding barrier distribution, have been measured and analyzed for several reactions involving ${}^{6,7}\text{Li}$. The results show that the effects of coupling to break-up channels are large for ${}^6\text{Li}$ and smaller for ${}^7\text{Li}$.

Recently, a systematic study of the ${}^{6,7}\text{Li} + {}^{64}\text{Zn}$ collisions at energies around the Coulomb barrier has been performed [15–17]. In Ref. [15], the elastic scattering of ${}^6\text{Li}$ on ${}^{64}\text{Zn}$ at



energies around the Coulomb barrier has been investigated within the optical model. The energy dependence of the optical potential shows absence of the usual threshold anomaly for the system ${}^6\text{Li}+{}^{64}\text{Zn}$. This new kind of anomaly is known as break-up threshold anomaly and it can be understood as an evidence of the effect of the coupling to the break-up channel.

Moreover, for the systems ${}^{6,7}\text{Li} + {}^{64}\text{Zn}$ the QEL and elastic excitation functions were measured and the corresponding barrier distributions were derived [16]. Coupled-channel calculations, including inelastic excitation of the projectile and target, do not reproduce the experimental data for the ${}^6\text{Li}$ system. This result suggests that the effects of couplings to the continuum are important in the reactions induced by ${}^6\text{Li}$. Therefore, to extend the coupled-channel calculations including the continuum states of the projectile and to investigate in detail the effects of such couplings, Continuum-Discretized Coupled-Channel (CDCC) calculations have been performed and presented in this contribution.

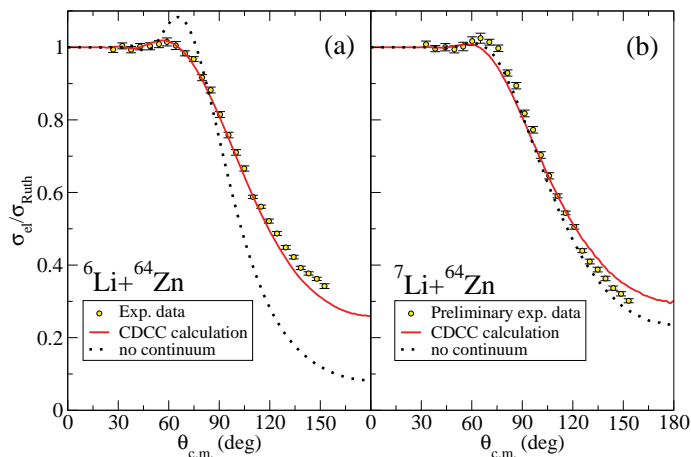


Figure 1. (Color online) Elastic scattering angular distribution for the reactions ${}^6\text{Li}+{}^{64}\text{Zn}$ (a) and ${}^7\text{Li}+{}^{64}\text{Zn}$ (b) at the same center of mass energy of 13.5 MeV. The CDCC calculations are represented by solid red lines, while the same calculations without the continuum couplings are shown by dotted black lines.

2. Experimental set-up and results

The experiments were performed at the Laboratori Nazionali del Sud, INFN, in Catania, Italy. The ${}^6\text{Li}$ and ${}^7\text{Li}$ beams were produced by the SMP Tandem Van de Graaff accelerator. Elastic-scattering angular distributions were measured at $E_{lab}=12\text{--}22$ MeV for the ${}^6\text{Li}+{}^{64}\text{Zn}$ system and at $E_{lab}=13\text{--}20$ MeV for ${}^7\text{Li}+{}^{64}\text{Zn}$. The target was a $400\ \mu\text{g}/\text{cm}^2$ thick ${}^{64}\text{Zn}$ foil in the ${}^6\text{Li}+{}^{64}\text{Zn}$ measurement. ${}^{64}\text{Zn}$ targets with thicknesses of $90\text{--}140\ \mu\text{g}/\text{cm}^2$, made by evaporation onto a carbon backing, were used for the measurements with ${}^7\text{Li}$. Outgoing charged particles were detected and charge identified by an array of five silicon telescopes. Each telescope consisted of a $10\ \mu\text{m}$ thick ΔE detector and an E detector with a thickness in the range $100\text{--}500\ \mu\text{m}$. The telescopes were mounted on a rotating plate in the CT2000 scattering chamber (see Ref. [15] for more details).

The measurements of the QEL scattering for the ${}^{6,7}\text{Li}+{}^{64}\text{Zn}$ systems were performed in the energy range $E_{lab}=9\text{--}20$ MeV in steps of 0.5 MeV. In this case, four silicon telescopes were positioned at $\pm 160^\circ$ and $\pm 170^\circ$ relative to the beam direction. ${}^{64}\text{Zn}$ targets with thicknesses of $140\ \mu\text{g}/\text{cm}^2$ and $70\ \mu\text{g}/\text{cm}^2$, evaporated onto a $15\ \mu\text{g}/\text{cm}^2$ carbon backing, were used for the measurements with ${}^6\text{Li}$ and ${}^7\text{Li}$, respectively (more experimental details can be found in Ref. [16]).

Experimental results for the ${}^6\text{Li}+{}^{64}\text{Zn}$ elastic scattering and for the ${}^{6,7}\text{Li}+{}^{64}\text{Zn}$ QEL backscattering have already been reported in Refs. [15] and [16], respectively. As an example, the elastic scattering angular distribution at $E_{c.m.}=13.5$ MeV for ${}^6\text{Li}$ [15] is shown in Fig. 1(a), while in Fig. 1(b) the experimental data for ${}^7\text{Li}$ at the same energy are presented.

In Ref. [16], in the case of the ${}^7\text{Li}+{}^{64}\text{Zn}$ system, the QEL scattering was defined as the sum of the elastic scattering, inelastic excitation of the ${}^7\text{Li}$ $1/2^-$ and ${}^{64}\text{Zn}$ 2^+ states, and 1n transfer to the ${}^{65}\text{Zn}$ states. In the case of ${}^6\text{Li}+{}^{64}\text{Zn}$, the elastic scattering and inelastic excitation of the ${}^{64}\text{Zn}$ 2^+ state were included in the QEL scattering. In this paper, we will focus on the elastic backscattering excitation functions and the corresponding contributions to the QEL barrier distributions.

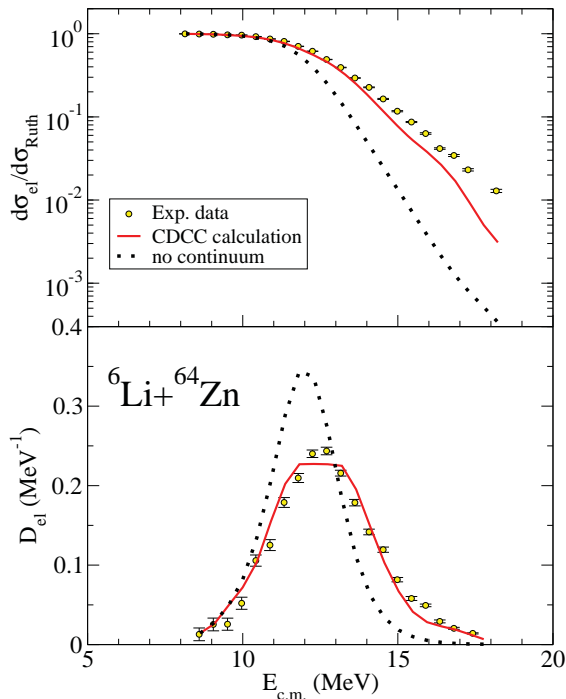


Figure 2. (Color online) Elastic excitation function at backward angles (top) and the corresponding barrier distribution (bottom) for the system ${}^6\text{Li}+{}^{64}\text{Zn}$. The experimental data are represented by the yellow symbols, while the solid red lines correspond to the CDCC calculations. The dotted black lines represent the calculations without the couplings to the continuum states.

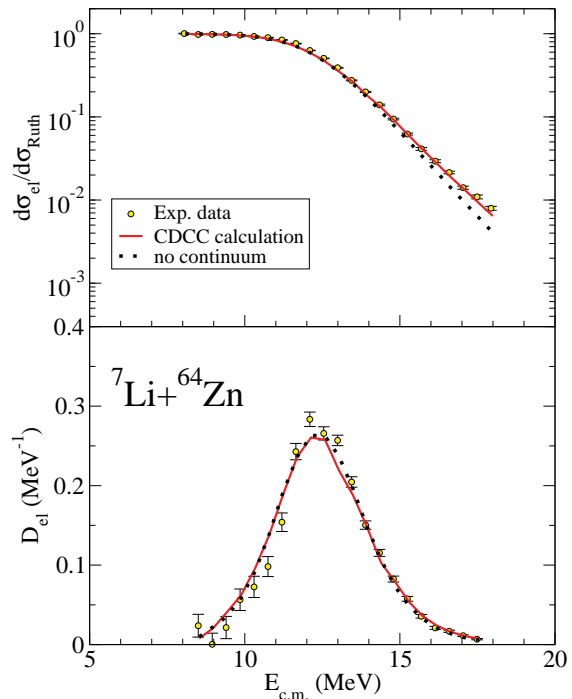


Figure 3. (Color online) Elastic excitation function at backward angles (top) and the corresponding barrier distribution (bottom) for the system ${}^7\text{Li}+{}^{64}\text{Zn}$. The experimental data are represented by the yellow symbols, while the solid red lines correspond to the CDCC calculations. The dotted black lines represent the calculations without the couplings to the continuum states.

3. Continuum-Discretized Coupled-Channels calculations

In the last years, the Continuum-Discretized Coupled-Channels (CDCC) method has been applied to describe reactions induced by weakly bound nuclei, using a three-body model of the reaction [18–21]. This formalism uses the coupled channel method to solve the scattering problem. It is known that for weakly bound nuclei it is important to take into account the continuum states of the projectile. These states are included and discretized by means of the so-called *binning* method [22].

In this framework, a three-body model of the reactions ${}^{6,7}\text{Li}+{}^{64}\text{Zn}$ ($\alpha+d(t)+{}^{64}\text{Zn}$) is considered. The ${}^6\text{Li}$ can be considered as having an $\alpha+d$ cluster structure, with a break-up threshold at 1.47 MeV above the ground state. The resonances 3^+ , 2^+ , 1^+ and the non-resonant

states are included in the calculations. On the other hand, the ${}^7\text{Li}$ isotope can be described as a $\alpha+t$, with a break-up threshold at 2.47 MeV. The excited state $1/2^-$, the resonances $7/2^-$, $5/2^-$ and the non-resonant states are considered. Both Coulomb and nuclear effects are included. These calculations were performed using the code FRESKO [23].

The calculated elastic scattering angular distributions for both systems are represented in Fig. 1. A good agreement between the prediction of the CDCC calculations and the experimental data is observed. To study the effects of the coupling to the continuum states of the projectile, we have included the calculations without such couplings, represented by the dotted black lines in Fig. 1. These calculations underestimate the experimental data for the ${}^6\text{Li}$ case, which suggests a strong coupling to the break-up channel in the ${}^6\text{Li}$ system.

In addition, the experimental elastic scattering excitation functions and the corresponding barrier distributions for ${}^6\text{Li}$ and ${}^7\text{Li}$ are compared with the CDCC calculations in Figs. 2 and 3. The calculations are also compared with those omitting the couplings to the continuum states of the projectile. The results show an important influence of the coupling to the break-up channel in the reactions induced by the ${}^6\text{Li}$ nucleus, while in the reaction induced by ${}^7\text{Li}$ small changes are observed. As it can be seen in Fig. 2, the effect of the coupling to the break-up channel is to increase the average barrier.

4. Conclusions

Experimental results for the ${}^{6,7}\text{Li}+{}^{64}\text{Zn}$ reactions at energies around the Coulomb barrier have been studied within the CDCC framework. The elastic scattering angular distributions are compared with the calculations, showing that it is necessary to include the couplings to continuum states of the projectile to reproduce the experimental data for the ${}^6\text{Li}$ reaction.

Moreover, the elastic excitation functions and the corresponding barrier distributions are well reproduced by the CDCC calculations. The results suggest that the coupling to the breakup channel is more relevant in the ${}^6\text{Li}$ induced collisions than in the ${}^7\text{Li}$ case. This behavior could be linked to the fact that the break-up threshold of ${}^6\text{Li}$ ($S_\alpha=1.47$ MeV) is smaller than that of ${}^7\text{Li}$ ($S_\alpha=2.47$ MeV).

References

- [1] Canto L F *et al.* 2006 *Phys. Rep.* **424** 1
- [2] Di Pietro A *et al.* 2010 *Phys. Rev. Lett.* **105** 022701
- [3] Fernández-García J P *et al.* 2010 *Nucl. Phys. A* **840** 19–38
- [4] Cubero M *et al.* 2012 *Phys. Rev. Lett.* **109** 262701
- [5] Canto L F *et al.* 2009 *Nucl. Phys. A* **821** 51
- [6] Scuderi V *et al.* 2011 *Phys. Rev. C* **84** 064604
- [7] Dasgupta M *et al.* 1998 *Annu. Rev. Nucl. Sci.* **48** 401
- [8] Lubian J *et al.* 2008 *Phys. Rev. C* **78**(6) 064615
- [9] Zagrebaev V I 2008 *Phys. Rev. C* **78**(4) 047602
- [10] Timmers H *et al.* 1995 *Nuclear Physics A* **584** 190 – 204
- [11] Mukherjee S *et al.* 2009 *Phys. Rev. C* **80**(1) 014607
- [12] Otomar D R *et al.* 2009 *Phys. Rev. C* **80**(3) 034614
- [13] Zerva K *et al.* 2009 *Phys. Rev. C* **80**(1) 017601
- [14] Zerva K *et al.* 2012 *Eur. Phys. J. A* **48** 102
- [15] Zadro M *et al.* 2009 *Phys. Rev. C* **80** 064610
- [16] Zadro M *et al.* 2013 *Phys. Rev. C* **87** 054606
- [17] Di Pietro A *et al.* 2013 *Phys. Rev. C* **87** 064614
- [18] Sakuragi Y 1987 *Phys. Rev.* **C35** 2161
- [19] Tostevin J A *et al.* 2001 *Phys. Rev. C* **63** 024617
- [20] Matsumoto T *et al.* 2003 *Phys. Rev. C* **68** 064607
- [21] Beck C *et al.* 2007 *Phys. Rev. C* **75** 054605
- [22] Austern N *et al.* 1987 *Physics Reports* **154** 125
- [23] Thompson I 1988 *Comp. Phys. Rep.* **7**, 167